Positioning with Starlink LEO Satellites: A Blind Doppler Spectral Approach

Sharbel E. Kozhaya and Zaher M. Kassas
Department of Electrical and Computer Engineering, The Ohio State University, Columbus, OH, USA
Emails: kozhaya.1@osu.edu and zkassas@ieee.org

***Abstract*—A blind Doppler spectral approach is proposed for exploiting *unknown* Starlink low Earth orbit (LEO) satellite signals for positioning. First, an analytical derivation of the received signal frequency spectrum is presented, which accounts for the highly dynamic channel between the LEO satellite and a ground-based receiver. Second, a frequency domain-based blind Doppler discriminator is proposed. Third, a Kalman filter (KF)-based Doppler tracking algorithm is developed. Finally, experimental results are presented of a stationary receiver tracking the Doppler, in a blind fashion, of six Starlink LEO satellites over a period of about 800 seconds with Hz-level accuracy. The Doppler measurements were fused through a nonlinear least-squares estimator to localize the receiver to an unprecedented level of accuracy. Starting with an initial estimate 200 km away, the proposed approach achieved a final horizontal two-dimensional (2D) position error of 4.3 m.**

***Index Terms*—Positioning, navigation, signals of opportunity, blind Doppler tracking, low Earth orbit satellite.**

I. Introduction

Global navigation satellite systems (GNSS) are at the core of modern navigation systems. GNSS receivers are routinely used to navigate today's ground and aerial vehicles and are embedded into mass marketed consumer devices (smart phones, watches, notepads, etc.) [1]. However, GNSS signals are prone to multipath and interference [2]. There has been a considerable effort recently to exploit ambient radio frequency (RF) signals of opportunity as complement or alternative to GNSS signals. These signals range from terrestrial sources (e.g., cellular [3], [4] and digital television [5], [6]) to extraterrestrial sources (e.g., low Earth orbit (LEO) [7], [8] and geostationary Earth orbit (GEO) [9] satellites).

The past few years ushered the new era of LEO megaconstellations, where thousands of LEO space vehicles (SVs) have been launched and tens of thousands scheduled for launch [10]. Using broadband LEO SV signals for navigation offers several desirable attributes [11], [12]: (i) higher received signal power compared to GNSS SVs that reside in medium Earth orbit (MEO), (ii) high availability and favorable geometry, and (iii) spectral diversity in the RF spectrum. However, using broadband LEO SV signals for navigation purposes comes with challenges [13], [14], as they are owned by private operators that typically do not disclose crucial information about the SVs': (i) ephemerides, (ii) clock synchronization and stability, and (iii) signal specifications.

To address the first challenge, several approaches have been recently proposed, including differential navigation utilizing a known base receiver [15], [16], simultaneous tracking and navigation (STAN) [17], and analytical/machine-learning SV orbit tracking [18], [19]. Approaches to address the second challenge have been offered in [20], [21]. To address the third challenge, the paradigm of cognitive opportunistic navigation, which estimates the minimally known LEO SV signals in a blind fashion has been showing tremendous promise [22], [23]. Most recently, this paradigm allowed for the exploitation of unknown Starlink LEO SVs, from which navigation observables were produced via (i) a carrier phase tracking approach [24] and (ii) a generalized likelihood ratio (GLR) Doppler detection approach [25], with the former localizing a receiver to within a two-dimensional (2D) error of 25.9 m, while the latter achieving a 2D error of 10 m.

This paper proposes a novel blind Doppler spectral approach to address the first challenge without the need to know the LEO SVs' donwlink signal specification. While the method is generalizable to any LEO constellation, Starlink SVs are chosen to demonstrate the proposed method's efficacy. Previous literature has proposed methods for Doppler tracking with M-ary phase shift keying (M-PSK) and orthogonal frequency division multiplexing (OFDM) signals [26]–[30]. The aforementioned approaches aim to generate a peak in the frequency-domain by either relying on nonlinear operations (for M-PSK signals) or increasing the coherent processing interval (CPI) (for OFDM signals). After generating the peak, the methods track it using a peak tracking algorithm to estimate the Doppler shift. However, using nonlinear operations could degrade the signal-to-noise ratio (SNR), while increasing the CPI is not straightforward with the highly dynamic channels encountered with LEO SVs. Also, peak tracking is prone to generate invalid observables and even divergence whenever the spectrum is contaminated by noisy DC peaks.

This paper proposes a novel approach to mitigate the above challenges and offers the following contributions: (i) derive an analytical approximation of the received signal frequency spectrum for highly dynamic channels and (ii) develop a blind Doppler spectral estimator via frequency-domain cross-correlation and a Kalman filter (KF)-based tracking loop. The proposed approach relies on the presence of a repetitive sequence in the LEO SV's downlink, to which the blind spectral Doppler tracker locks and cross-correlation is used to track the Doppler shift. While spectral cross-correlation has been studied in the literature [31] and used for noise reduction in speech [32] and detection of stars and planets [33], to the author's knowledge, this approach is newly applied

to tracking the Doppler of LEO SVs. Experimental results with six Starlink SVs are presented showing the superiority of the proposed approach over state-of-the-art blind positioning methods. The proposed approach yielded an unprecedented Hz-level Doppler tracking accuracy and 2D positioning error of 4.3 m, which is 57% lower than the most accurate results with Starlink reported in the literature to-date.

This paper is organized as follows. Section II derives the signal model. Section III introduces the blind Doppler discriminator and tracking approach. Section IV presents experimental results. Section V gives concluding remarks.

II. Signal Model

This section presents a model of the received signal, which takes into account the high dynamics channel between the LEO SV and ground-based receiver. Then, it derives an analytical expression of the signal's frequency spectrum.

A. Received Baseband Signal Model

Let $x(t)$ be the unknown LEO SV signal, expressed at baseband. The proposed framework does not assume any particular modulation or multiplexing scheme. The only assumption is that $x(t)$ can be written as $x(t) = s(t) + n_d(t)$, where $s(t)$ is a deterministic repetitive signal and $n_d(t)$ is a random signal driven by the user data. Examples of repetitive sequences are the pseudorandom noise (PRN) used in GPS [34], Globalstar LEO SVs [35], and CDMA2000 [36] and the primary and secondary synchronization sequences (PSS and SSS) used in 4G long-term evolution (LTE) [37] and 5G [38]. The proposed framework assumes the following properties of $s(t)$:

1) It is periodic with period T_0.
2) It is uncorrelated with the data $n_d(t)$.
3) It is zero-mean, has a stationary power spectral density (PSD) with $\left|\mathcal{F}\left\{s(t)w_{T_0}(t)\right\}\right|^2 = S_s(f)$, where $w_{T_0}(t)$ is a windowing function that is unity within the interval $[0, T_0]$ and zero elsewhere.

Consider $x(t)$ being transmitted at a carrier frequency f_c. Let $\tau_d(t)$ denote the apparent delay between the transmitted signal $x_c(t) \triangleq x(t)\exp(j2\pi f_c t)$ and the received signal at the receiver's antenna. The apparent delay $\tau_d(t)$ is composed of (i) the time-of-flight along the line-of-sight (LOS) between the transmitter and receiver (i.e., $d_{LOS}(t)/c$, where $d_{LOS}(t)$ is the LOS distance between the LEO SV's transmitter and the receiver and c is the speed of light); (ii) combined effect of the transmitter's and receiver's clock biases, denoted $\delta t_{clk}(t)$; (iii) ionospheric and tropospheric delays $\delta t_{iono}(t)$ and $\delta t_{tropo}(t)$, respectively; and (iv) other unmodeled errors. After propagating in an additive white Gaussian channel, the resulting received signal before baseband mixing can be expressed as

$$\begin{aligned}\bar{r}(t) &= x_c\left(t - \tau_d(t)\right) + \bar{n}(t) \\ &= x(t - \tau_d(t))\exp\left(j2\pi f_c\left[t - \tau_d\left(t\right)\right]\right) + \bar{n}(t),\end{aligned}$$

where $\bar{n}(t)$ is a complex white Gaussian noise with PSD $N_0/2$.

Let $r(t) \triangleq \bar{r}(t)\exp\left(-j2\pi f_c t\right)$ denote the received signal after baseband mixing and filtering. Then, $r(t)$ can be expressed as $r(t) = x(t - \tau_d(t))\exp\left(j\theta(t)\right) + n(t)$, where $n(t)$ is the low-pass filter output of $\bar{n}(t)$, and $\theta(t) = -2\pi f_c \tau_d(t)$ is the carrier phase of the received signal. Using a Taylor series expansion, at time instant $t_k = t_0 + kT_0$, where k is the sub-accumulation index and t_0 is some initial time, the carrier phase of the signal can be expressed as

$$\theta(t) = \theta(t_k) + \dot{\theta}(t_k)t + \frac{1}{2}\ddot{\theta}(t_k)t^2 + H.O.T. \tag{1}$$

Denote $\theta_k(t)$ as $\theta(t)$ in (1), after dropping the higher-order terms ($H.O.T.$). By definition, $f_D(t) \triangleq \frac{\dot{\theta}(t)}{2\pi}$ is the apparent Doppler shift and $\dot{f}_D(t)$ is the apparent Doppler rate.

It is important to note that the channel between the LEO SV and the ground-based receiver is highly dynamic, thus, high Doppler shift and rate will be observed by the receiver. On the other hand, at the k-th sub-accumulation, $\tau_d(t)$ is approximated by its zero-order term $d_k = \tau_d(t_k)$, while the higher order terms are dropped to simplify the following signal analysis. Due to the first property, one can arbitrarily choose $\tau_d(t)$ to denote the code start time. It is important to note that the higher order terms in $\tau_d(t)$ stretch or contract the code in the time-domain, but this paper ignores this effect, which seems to be of little impact on Starlink LEO SV codes.

Finally, the expression of the received signal at the k-th sub-accumulation can be written as $r_k^-(t) = r(t)w_{T_0}(t - t_k) = s_k(t)\exp\left(j\theta_k(t)\right) + n_k^-(t)$, where $s_k(t) = s(t - d_k)w_{T_0}(t)$ and $n_k^-(t) = n(t - d_k)w_{T_0}(t)$. The received signal $r_k(t)$ after carrier wipe-off using the carrier phase estimate, denoted $\hat{\theta}_k(t)$, generated by the tracking loop discussed in Section III-B, can be expressed as

$$\begin{aligned}r_k(t) &= r_k^-(t)\exp(-j\hat{\theta}_k(t)) \\ &= s_k(t)\exp(j\tilde{\theta}_k(t)) + n_k(t),\end{aligned} \tag{2}$$

where $\tilde{\theta}_k(t) = \theta_k(t) - \hat{\theta}_k(t)$ is the residual carrier phase.

B. Frequency Spectrum of the Received Signal

The received signal's frequency spectrum at the k-th sub-accumulation is $S_{r_k}(f) = \left|\mathcal{F}\left\{r_k(t)\right\}\right|^2$. Using the third property of $s(t)$, the Wigner distribution function (WDF) of $s_k(t)$ for $t \in [0, T_0]$ can be written as

$$\begin{aligned}W_s(t, f) &\triangleq \int_{-\infty}^{\infty} s_k\left(t + \frac{\tau}{2}\right) s_k^*\left(t - \frac{\tau}{2}\right)\exp(-2\pi f\tau)\, d\tau \\ &= \frac{S_s(f)}{T_0}.\end{aligned}$$

It can be shown that the WDF of the residual carrier phase at the k-th sub-accumulation $C_k(t) = \exp(j\tilde{\theta}_k(t))$, for $t \in [0, T_0]$, is $W_{C_k}(t, f) = \delta\left(f - \frac{\dot{\tilde{\theta}}_k}{2\pi} - \frac{\ddot{\tilde{\theta}}_k}{2\pi}t\right)$, where $\delta(\cdot)$ denotes the Dirac delta function. Using the second property of $s(t)$, the WDF of $r_k(t)$ in (2), for $t \in [0, T_0]$, can be written as

$$W_{r_k}(t, f) = \frac{S_s(f)}{T_0} \circledast \delta\left(f - \frac{\dot{\tilde{\theta}}_k}{2\pi} - \frac{\ddot{\tilde{\theta}}_k}{2\pi}t\right) + W_{n_k}(t, f),$$

where $(f \circledast g)(t) = \int_{-\infty}^{\infty} f(\tau)g(t - \tau)d\tau$ is the convolution, $W_{n_k}(t, f)$ is the WDF of the noise and data at the k-th sub-accumulation. Noting that $S_{r_k}(f) = \int_0^{T_0} W_{r_k}(t, f)\, dt$ and using the projection property of WDF, the following follows

$$S_{r_k}(f) = \frac{S_s(f)}{T_0} \circledast \int_0^{T_0} \delta\left(f - \frac{\tilde{\dot\theta}_k}{2\pi} - \frac{\tilde{\ddot\theta}_k}{2\pi} t\right) dt + S_{n_k}(f)$$
$$= S_s(f) \circledast \frac{2\pi}{\left|\tilde{\ddot\theta}_k\right| T_0} \int_0^{T_0} \delta\left(t - \frac{2\pi f - \tilde{\dot\theta}_k}{\tilde{\ddot\theta}_k}\right) dt + S_{n_k}(f)$$
$$= S_s(f) \circledast \Pi\left(f; \tilde{\dot\theta}_k, \tilde{\ddot\theta}_k\right) + S_{n_k}(f), \tag{3}$$

where $S_{n_k}(f) = \int_0^{T_0} W_{n_k}(t,f)\, dt$ and

$$\Pi\left(f; \dot\theta, \ddot\theta\right) = \frac{2\pi}{\left|\ddot\theta\right| T_0} \begin{cases} 1, & \left| f - \dfrac{\dot\theta + \dfrac{|\ddot\theta|}{2} T_0}{2\pi} \right| < \dfrac{|\ddot\theta|}{4\pi} T_0, \\ 0, & \text{elsewhere.} \end{cases}$$

Equation (3) states that the received signal's frequency spectrum consists of a shifted and dilated version of the repetitive sequence's frequency spectrum alongside a noise floor. The shifting in the received spectrum is mainly due to residual Doppler $\tilde{\dot\theta}_k$ and the dilation is due to residual Doppler rate $\tilde{\ddot\theta}_k$.

III. Blind Doppler Tracking

This section derives the Doppler discriminator and formulates the KF-based Doppler tracking loop.

A. Frequency-Domain Based Doppler Discriminator

The nonlinear least-squares (NLS) estimator of the residual Doppler $\tilde{\dot\theta}_k$ at the k-th sub-accumulation is given by

$$\tilde{\dot\theta}_k = \underset{\dot\theta}{\operatorname{argmin}} \left\| S_{r_k}(f) - S_s(f) \circledast \Pi\left(f; \dot\theta, \ddot\theta\right) \right\|^2$$
$$= \underset{\dot\theta}{\operatorname{argmin}} \left\| S_{r_k}(f) \right\|^2 + \left\| S_s(f) \circledast \Pi\left(f; \dot\theta, \ddot\theta\right) \right\|^2$$
$$- 2\left(S_{r_k} \star S_s\right)(f) \circledast \Pi\left(f; \dot\theta, \ddot\theta\right) \tag{4}$$
$$= \underset{\dot\theta}{\operatorname{argmax}} \left(S_{r_k} \star S_s\right)(f) \circledast \Pi\left(f; \dot\theta, \ddot\theta\right)$$
$$\approxeq \underset{\dot\theta}{\operatorname{argmax}} \left(S_{r_k} \star S_s\right)(f) \circledast \delta\left(f - \frac{\dot\theta}{2\pi}\right), \quad \text{for} \quad \tilde{\ddot\theta}_k \approx 0$$
$$= 2\pi \underset{f}{\operatorname{argmax}} \left(S_{r_k} \star S_s\right)(f), \tag{5}$$

where $(f \star g)(\tau) = \int_{-\infty}^{\infty} f^*(t) g(t+\tau) dt$ is the cross-correlation. The first two terms in the minimization problem (4) are a constant function of the search parameter $\dot\theta$; therefore, they are ignored. As the blind receiver does not have prior knowledge of $S_s(f)$, it starts with an initial estimate $\hat{S}_s(f) \triangleq S_{r_0}(f)$ and refines the repetitive sequence's spectrum with every sub-accumulation. It is worth pointing that the regime of small residual Doppler rate values assumed in (5) is a reasonable assumption, since the Doppler rate between two consecutive sub-accumulations is nearly constant.

B. Kalman Filter-Based Tracking Loop

The continuous-time signal in (2) is sampled at a sampling interval $T_s = 1/F_s$, the discrete-time received signal before carrier wipe-off at the k-th sub-accumulation can be written as

$$r_k^-[n] = s[n - d_k] \exp\left(j\tilde{\Theta}_k[n]\right) + n_k^-[n],$$

where $n \in [0, L-1]$, $s[n]$ is the discrete-time sequence of $s(t)$ with period $L = T_0/T_s$ and $\tilde{\Theta}_k[n]$ and d_k are the discrete-time carrier phase and code start time, respectively, of the received signal at the k-th sub-accumulation.

The carrier phase state vector is defined as $\boldsymbol{\theta}(t) \triangleq \left[\theta(t),\ \dot\theta(t),\ \ddot\theta(t)\right]^{\mathsf{T}}$, whose dynamics is modeled as

$$\dot{\boldsymbol{\theta}}(t) = \mathbf{A}\boldsymbol{\theta}(t) + \mathbf{B}\boldsymbol{w}(t), \tag{6}$$
$$\mathbf{A} \triangleq \begin{bmatrix} 0 & 1 & 0 \\ 0 & 0 & 1 \\ 0 & 0 & 0 \end{bmatrix}, \quad \mathbf{B} \triangleq \begin{bmatrix} 0 \\ 0 \\ 1 \end{bmatrix},$$

where $\boldsymbol{w}(t)$ is a zero-mean white noise process with power spectral density q_w. The continuous-time dynamics in (6) is discretized at a sampling time $T_0 = LT_s$, leading to $\boldsymbol{\Theta}_{k+1} = \mathbf{F}\boldsymbol{\Theta}_k + \mathbf{w}_k$, where $\boldsymbol{\Theta}_k \triangleq \left[\theta_k,\ \dot\theta_k,\ \ddot\theta_k\right]^{\mathsf{T}}$, $\mathbf{F} \triangleq e^{\mathbf{A}T_0}$ is the state transition matrix, $\mathbf{w}_k$ is a discrete-time process noise vector, which is a zero-mean white sequence with covariance $\mathbf{Q} = q_{\tilde{w}} \int_0^{T_0} e^{\mathbf{A}t}\mathbf{B}\left(e^{\mathbf{A}t}\mathbf{B}\right)^{\mathsf{T}} dt$. The reconstructed sequence of the carrier phase used to perform carrier wipe-off can be written as a second order piecewise polynomial given by $\hat{\Theta}_k[n] = \hat\theta_{k-1} + \hat{\dot\theta}_k n T_s + \frac{1}{2}\hat{\ddot\theta}_k (nT_s)^2$, $n \in [0, L-1]$. After carrier wipe-off, the received signal's sequence can be expressed as

$$r_k[n] = s[n - d_k] \exp\left(j\tilde{\Theta}_k[n]\right) + n_k[n]. \tag{7}$$

Equation (7) will be used to determine the residual Doppler $\tilde{\dot\theta}_k$ at the k-th sub-accumulation, which is fed as innovation to a KF loop that uses the observation model $z_k = \mathbf{H}\boldsymbol{\Theta}_k + v_k$, where $\mathbf{H} \triangleq [0\ \ 1\ \ 0]$ and v_k is a discrete-time zero-mean white noise sequence with variance $\sigma_{\dot\theta}^2$. The KF innovation ν_k is the fast Fourier transform (FFT)-based discrete-time version of (5). It is worth noting that the Doppler tracked using the proposed approach has a real-valued ambiguity part $\dot\theta_N$ that needs to be resolved to retrieve back the actual Doppler shift.

IV. Experimental Results

This section demonstrates the proposed blind Doppler estimator and tracking loop with Starlink LEO SV signals. To this end, a stationary National Instrument (NI) universal software radio peripheral (USRP) 2945R was equipped with a consumer-grade Ku antenna and low-noise block (LNB) downconverter to receive Starlink signals in the Ku-band. The sampling bandwidth was set to 2.5 MHz and the carrier frequency f_c was set to 11.325 GHz. Samples of the Ku signal were stored for off-line processing via a software-defined radio (SDR). The experimental hardware is shown in Fig. 1.

Fig. 1. Experimental hardware.

A. Blind Doppler Tracking Results

The USRP was set to record Ku signals over a period of 800 seconds. During this period, a total of six Starlink SVs passed over the receiver, one at a time. The framework discussed in Section III was used to acquire and track the signals from these SVs with $q_w = (0.1)^2$ rad^2/s^6 and $\sigma_{\dot{\theta}} = \frac{\pi}{6}$ rad/s. The SVs' skyplot, time history of the KF innovation ν_k, and tracked Doppler shift $\hat{f}_{D_k} = \hat{\dot{\theta}}_k/2\pi$ for each SV is shown in Fig. 2.

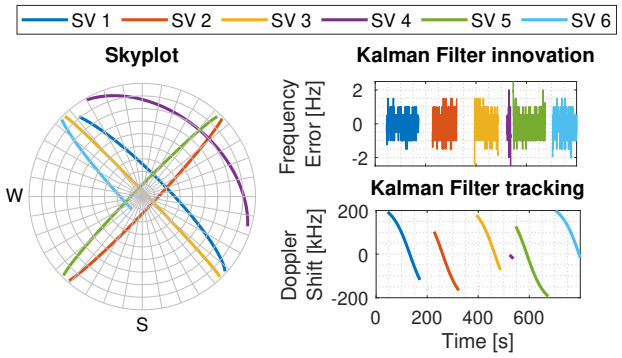

Fig. 2. Left: Skyplot of the six Starlink LEO SVs. Right: time history of the KF innovation ν_k and tracked Doppler shift $\hat{f}_{D_k}$ for each SV.

B. Position Solution

Let $i \in [1, 6]$ denote the SV index. The pseudorange rate observable $z^i(k) \triangleq c\frac{\hat{f}_{D_k}}{f_c}$ of the i-th SV at time-step k, expressed in meters, is modeled as

$$z^i(k) = \frac{\dot{\boldsymbol{r}}_{\mathrm{SV}_i}^{\mathsf{T}}(k)\left[\boldsymbol{r}_r - \boldsymbol{r}_{\mathrm{SV}_i}(k')\right]}{\|\boldsymbol{r}_r - \boldsymbol{r}_{\mathrm{SV}_i}(k')\|_2} + a_i + v_{z_i}(k), \qquad (8)$$

where $\boldsymbol{r}_r$ and $\boldsymbol{r}_{\mathrm{SV}_i}$ are the receiver's and i-th Starlink SV's 3D position vectors; $\dot{\boldsymbol{r}}_{\mathrm{SV}_i}$ is the i-th SV's 3D velocity vector; k' is the time at the i-th SV; a_i is a bias that models the (i) unknown Doppler ambiguity $\dot{\theta}_N$, (ii) lumped receiver–SV clock drift, and (iii) ionospheric and tropospheric delay rate; $v_{z_i}(k)$ is the measurement noise, which is modeled as a zero-mean, white Gaussian random sequence with variance σ_i^2.

Next, define the parameter vector $\boldsymbol{x} \triangleq \left[\boldsymbol{r}_r{}^{\mathsf{T}}, a_1, \ldots, a_6\right]^{\mathsf{T}}$. Let $\boldsymbol{z}$ denote the vector of all the pseudorange observables stacked together, and let $\boldsymbol{v}_z$ denote the vector of all measurement noises stacked together. Then, one can readily write the measurement equation given by $\boldsymbol{z} = \boldsymbol{g}(\boldsymbol{x}) + \boldsymbol{v}_z$, where $\boldsymbol{g}(\boldsymbol{x})$ is a vector-valued function that maps the parameter $\boldsymbol{x}$ to the pseudorange rate observables according to (8). Next, an NLS estimator is used to obtain an estimate of $\boldsymbol{x}$. The SV positions were obtained from TLE files and SGP4 orbit propagator. It is important to note that the TLE epoch time was adjusted for each SV to account for ephemeris errors. This was achieved by minimizing the pseudorange rate residuals for each SV. Subsequently, the receiver position was estimated using the aforementioned NLS. The receiver position was initialized 200 km away from the true position. The final 3D position error was found to be 19.4 m, while the horizontal 2D position error was 4.3 m. The results are summarized in Fig. 3.

Table I compares the results achieved with the proposed approach against the only positioning results with Starlink LEO SV signals reported in the literature. Using the same recorded samples from Starlink SVs in [24], [25], the proposed approach reduced the 3D and 2D positioning error by 15.3% and 57%, respectively, over the most accurate positioning results with Starlink reported in the literature to-date.

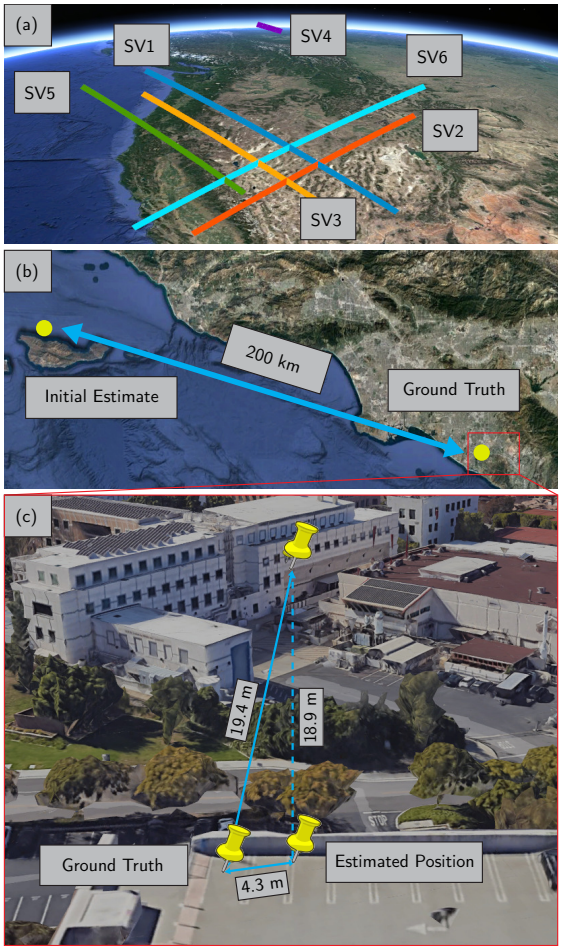

Fig. 3. Environment layout summarizing the positioning results

TABLE I
COMPARISON OF STARLINK POSITIONING RESULTS.

	Carrier phase [24]	GLR Doppler [25]	Proposed approach
3D error (m)	33.5	22.9	19.4
2D error (m)	25.9	10.0	4.3

V. CONCLUSION

This paper proposed a novel approach for blind Doppler tracking of LEO SVs. First, an analytical expression for the received signal frequency spectrum was derived, which accounts for high LEO SVs' dynamic channels. Second, a novel frequency-domain-based Doppler discriminator was proposed. Third, a KF-based Doppler tracking algorithm was developed. Finally, experimental results were presented showing Hz-level Doppler tracking of six Starlink LEO SV signals. Starting with an initial estimate 200 km away, the proposed approach achieved a 2D error of 4.3 m.

ACKNOWLEDGMENTS

The authors thank Dr. Joe Khalife for his help with data collection. This work was supported in part by the Office of Naval Research (ONR) under Grants N00014-19-1-2511 and N00014-22-1-2242 and in part by the U.S. Department of Transportation (USDOT) under Grant 69A3552047138 for the CARMEN University Transportation Center (UTC).

REFERENCES

[1] N. Gogoi, A. Minetto, and F. Dovis, "On the cooperative ranging between Android smartphones sharing raw GNSS measurements," in *Proceedings of IEEE Vehicular Technology Conference*, 2019, pp. 1–5.

[2] S. Sand, P. Unterhuber, D. B. Ahmed, F. Muller, A. Lehner, I. Rashdan, M. Schmidhammer, R. Karasek, B. Siebler, O. Heirich, C. Gentner, M. Walter, S. Kaiser, M. Ulmschneider, M. Schaab, L. Wientgens, and T. Strang, "Radio interference measurements for urban cooperative intelligent transportation systems," in *Proceedings of IEEE Vehicular Technology Conference*, 2021, pp. 1–6.

[3] R. Whiton, J. Chen, T. Johansson, and F. Tufvesson, "Urban navigation with LTE using a large antenna array and machine learning," in *Proceedings of IEEE Vehicular Technology Conference*, 2022, pp. 1–5.

[4] I. Lapin, G. Granados, J. Samson, O. Renaudin, F. Zanier, and L. Ries, "STARE: Real-time software receiver for LTE and 5G NR positioning and signal monitoring," in *Proceedings of Workshop on Satellite Navigation Technology*, April 2022, pp. 1–11.

[5] N. Souli, R. Makrigiorgis, P. Kolios, and G. Ellinas, "Cooperative relative positioning using signals of opportunity and inertial and visual modalities," in *Proceedings IEEE Vehicular Technology Conference*, 2021, pp. 1–7.

[6] Z. Jiao, L. Chen, X. Lu, Z. Liu, X. Zhou, Y. Zhuang, and G. Guo, "Carrier phase ranging with DTMB signals for urban pedestrian localization and GNSS aiding," *Remote Sensing*, vol. 15, no. 2, pp. 423–446, 2023.

[7] N. Jardak and Q. Jault, "The potential of LEO satellite-based opportunistic navigation for high dynamic applications," *Sensors*, vol. 22, no. 7, pp. 2541–2565, 2022.

[8] M. Hartnett, "Performance assessment of navigation using carrier Doppler measurements from multiple LEO constellations," Master's thesis, Air Force Institute of Technology, Ohio, USA, 2022.

[9] Y. Gao, X. Zhao, S. Wang, Y. Xiang, C. Huang, and Y. Hua, "Positioning via GEO communication satellites' signals of opportunity," *IET Radar, Sonar Navigation*, vol. 15, no. 11, pp. 1472–1482, July 2021.

[10] S. Liu, Z. Gao, Y. Wu, D. Kwan Ng, X. Gao, K. Wong, S. Chatzinotas, and B. Ottersten, "LEO satellite constellations for 5G and beyond: How will they reshape vertical domains?" *IEEE Communications Magazine*, vol. 59, no. 7, pp. 30–36, July 2021.

[11] T. Reid, T. Walter, P. Enge, D. Lawrence, H. Cobb, G. Gutt, M. O'Conner, and D. Whelan, "Position, navigation, and timing technologies in the 21st century," J. Morton, F. van Diggelen, J. Spilker, Jr., and B. Parkinson, Eds. Wiley-IEEE, 2021, vol. 2, ch. 43: Navigation from low Earth orbit – Part 1: concept, current capability, and future promise, pp. 1359–1379.

[12] Z. Kassas, "Position, navigation, and timing technologies in the 21st century," J. Morton, F. van Diggelen, J. Spilker, Jr., and B. Parkinson, Eds. Wiley-IEEE, 2021, vol. 2, ch. 43: Navigation from low Earth orbit – Part 2: models, implementation, and performance, pp. 1381–1412.

[13] Z. Kassas, M. Neinavaie, J. Khalife, N. Khairallah, J. Haidar-Ahmad, S. Kozhaya, and Z. Shadram, "Enter LEO on the GNSS stage: Navigation with Starlink satellites," *Inside GNSS Magazine*, vol. 16, no. 6, pp. 42–51, 2021.

[14] F. Prol, R. Ferre, Z. Saleem, P. Välisuo, C. Pinell, E. Lohan, M. Elsanhoury, M. Elmusrati, S. Islam, K. Celikbilek, K. Selvan, J. Yliaho, K. Rutledge, A. Ojala, L. Ferranti, J. Praks, M. Bhuiyan, S. Kaasalainen, and H. Kuusniemi, "Position, navigation, and timing (PNT) through low earth orbit (LEO) satellites: A survey on current status, challenges, and opportunities," *IEEE Access*, vol. 10, pp. 83 971–84 002, 2022.

[15] J. Khalife and Z. Kassas, "Performance-driven design of carrier phase differential navigation frameworks with megaconstellation LEO satellites," *IEEE Transactions on Aerospace and Electronic Systems*, pp. 1–20, 2023, accepted.

[16] C. Zhao, H. Qin, N. Wu, and D. Wang, "Analysis of baseline impact on differential doppler positioning and performance improvement method for LEO opportunistic navigation," *IEEE Transactions on Instrumentation and Measurement*, pp. 1–10, 2023.

[17] Z. Kassas, N. Khairallah, and S. Kozhaya, "Ad astra: Simultaneous tracking and navigation with megaconstellation LEO satellites," *IEEE Aerospace and Electronic Systems Magazine*, 2023, accepted.

[18] D. Shen, J. Lu, G. Chen, E. Blasch, C. Sheaff, M. Pugh, and K. Pham, "Methods of machine learning for space object pattern classification," in *Proceedings of IEEE National Aerospace and Electronics Conference*, 2019, pp. 565–572.

[19] J. Haidar-Ahmad, N. Khairallah, and Z. Kassas, "A hybrid analytical-machine learning approach for LEO satellite orbit prediction," in *Proceedings of International Conference on Information Fusion*, 2022, pp. 1–7.

[20] N. Khairallah and Z. Kassas, "An interacting multiple model estimator of LEO satellite clocks for improved positioning," in *Proceedings of IEEE Vehicular Technology Conference*, 2022, pp. 1–5.

[21] K. Wang and A. El-Mowafy, "LEO satellite clock analysis and prediction for positioning applications," *Geo-spatial Information Science*, vol. 25, no. 1, pp. 14–33, 2022.

[22] M. Neinavaie, J. Khalife, and Z. Kassas, "Blind Doppler tracking and beacon detection for opportunistic navigation with LEO satellite signals," in *Proceedings of IEEE Aerospace Conference*, 2021, pp. 1–8.

[23] S. Kozhaya and Z. Kassas, "Blind receiver for LEO beacon estimation with application to UAV carrier phase differential navigation," in *Proceedings of ION GNSS Conference*, 2022, pp. 2385–2397.

[24] J. Khalife, M. Neinavaie, and Z. Kassas, "The first carrier phase tracking and positioning results with Starlink LEO satellite signals," *IEEE Transactions on Aerospace and Electronic Systems*, vol. 56, no. 2, pp. 1487–1491, April 2022.

[25] M. Neinavaie, J. Khalife, and Z. Kassas, "Acquisition, Doppler tracking, and positioning with Starlink LEO satellites: First results," *IEEE Transactions on Aerospace and Electronic Systems*, vol. 58, no. 3, pp. 2606–2610, June 2022.

[26] Z. Tan, H. Qin, L. Cong, and C. Zhao, "New method for positioning using IRIDIUM satellite signals of opportunity," *IEEE Access*, vol. 7, pp. 83 412–83 423, 2019.

[27] F. Farhangian and R. Landry, "Multi-constellation software-defined receiver for Doppler positioning with LEO satellites," *Sensors*, vol. 20, no. 20, pp. 5866–5883, October 2020.

[28] C. Zhao, H. Qin, and Z. Li, "Doppler measurements from multiconstellations in opportunistic navigation," *IEEE Transactions on Instrumentation and Measurement*, vol. 71, pp. 1–9, 2022.

[29] C. Huang, H. Qin, C. Zhao, and H. Liang, "Phase - time method: Accurate Doppler measurement for Iridium NEXT signals," *IEEE Transactions on Aerospace and Electronic Systems*, vol. 58, no. 6, pp. 5954–5962, 2022.

[30] J. Khalife, M. Neinavaie, and Z. Kassas, "Blind Doppler tracking from OFDM signals transmitted by broadband LEO satellites," in *Proceedings of IEEE Vehicular Technology Conference*, April 2021, pp. 1–6.

[31] T. Frederick, "Time-frequency estimation for cyclostationary signals," Ph.D. dissertation, Florida Atlantic University, USA, 1997.

[32] S. Vaseghi, *Advanced digital signal processing and noise reduction*. John Wiley & Sons, 2008.

[33] S. Zucker, "Cross-correlation and maximum-likelihood analysis: a new approach to combining cross-correlation functions," *Monthly Notices of the Royal Astronomical Society*, vol. 342, no. 4, pp. 1291–1298, 2003.

[34] A. Flores, "NAVSTAR GPS space segment/navigation user interfaces," https://www.gps.gov/technical/icwg/IS-GPS-200N.pdf, August 2022.

[35] R. Hendrickson, "Globalstar for the military," in *Proceedings of IEEE Military Communications Conference*, vol. 3, November 1997, pp. 1173–1178.

[36] 3GPP2, "Physical layer standard for cdma2000 spread spectrum systems (C.S0002-E)," 3rd Generation Partnership Project 2 (3GPP2), TS C.S0002-E, June 2011.

[37] 3GPP, "Evolved universal terrestrial radio access (E-UTRA); multiplexing and channel coding," 3rd Generation Partnership Project (3GPP), TS 36.212, January 2010. [Online]. Available: http://www.3gpp.org/ftp/Specs/html-info/36212.htm

[38] 3GPP, "Physical channels and modulation," https://www.etsi.org/deliver/etsi-ts/138200-138299/138211/15.02.00-60/ts-138211v150200p.pdf, 5G; NR; 3rd Generation Partnership Project (3GPP), TS 38.211, July 2018.